Eng. Sci., 2021, **15**, 197–209

Engineered Science

DOI: https://dx.doi.org/10.30919/es8e512

Distinctive Solvatochromic Response of Fluorescent Carbon Dots Derived from Different Components of Aegle Marmelos Plant

Anjali Vijeata,[1] Ganga Ram Chaudhary,[1*] Ahmad Umar[2, 3*] and Savita Chaudhary[1*]

Abstract

The phenomenal properties of carbon dots (CQDs) have provoked significant research interest in both theoretical and technological point of view. Herein a simple, inexpensive and eco-friendly approach was used for the fabrication of five different types of bright blue emitting CQDs from different fruit parts of *Aegle Marmelos*. The prepared particles possess average particle size of 5 to 10 nm and displayed higher quantum yield *i.e.* 62.1%, 40.1%, 41. 4%, 43.4% and 48.2% for CQD_1, CQD_2, CQD_3, CQD_4 and CQD_5 respectively. The prepared CQDs also acquired exclusive characteristic features, comprising of high solubility, low toxicity as well as solvent polarity-dependent absorption and emission behaviour. The developed CQDs displayed higher stability over a period of four months. The detailed studies of CQDs in different solvents were further used to apprehend the solvatochromic behaviour of developed CQDs which have rarely been investigated. The provenience of solvatochromic shifts in various solvents and their corresponding effect on emission spectra of asynthesised CQDs were unveiled by scrutinizing the emission properties of five different types of formed CQDs as excitation wavelength. A red shift of 47 nm, 41 nm, 40 nm, 36 nm and 35 nm was observed in the emission spectra of CQD_1 to CQD_5 on moving towards the polar medium. The consequence of different solvents on the emission centers of CQDs were thoroughly investigated by calculating the solvent $E_T(30)$ polarity parameter for all chosen solvents. This work could unlock a new horizon to fabricate ratiometric probes of carbon dots for checking solvent polarity.

Keywords: Carbon dots; *Aegle Marmelos;* solubility; solvatochromic; $E_T(30)$.
Received: 1 April 2021; Accepted date: 23 May 2021.
Article type: Research article.

1. Introduction

The widespread utilities of photoluminescent compounds in bio-imaging, photonic, sensing, and molecular tracing has made them most significant compounds in material science.[1-8] Among all available collection of photoluminescent compounds (commercial dyes, polymers, lanthanides, semiconducting nanoparticles), carbon based nanoparticles especially carbon dots (CQDs) have acquired huge curiosity among researchers.[9-12]

The ease of preparation in cost effective manner, higher structural stability in different environmental conditions with better control over the solubility and biocompatibility has made them useful fluorophore material.[13-18] Till date, CQDs have been synthesised by disintegrating the appropriate carbon source by variety of bottom up techniques involving thermal and microwave based heating methods.[19-24] For instance, Chauhan *et al.*[22] have described the large-scale synthetic procedure for converting biologically infected environmental pollutant *i.e.* agar gel waste into immensely fluorescent CQDs. The upcycling of single used plastic waste and conversion of natural precursors such as banana, rice husk, lychee seeds, orange peel, cotton, sugarcane into fluorescent CQDs have also been stated in literature.[25-30]

Recently, the fabrication of CQDs with multicolour fluorescent emission has generated immense interest among researchers.[31-34] The polarity of the chosen solvent has possessed significant effect on the emission colour of CQDs.[35-40] In addition, the optical properties of CQDs have also been influenced under different pH and temperature conditions.[41-44] Basu and Mandal described the effect of solvent on the emission properties of 4 nm sized CQDs.[45] Reckmeier and coworkers explained the solvatochromic shifts in PL bands of CQDs in presence of different solvents.[46] Stepanidenko *et al.*[47] investigated the influential effect of solvent environment on the physicochemical properties of

[1] *Department of Chemistry and Centre of Advanced Studies in Chemistry, Panjab University, Chandigarh 160014, India.*
[2] *Department of Chemistry, College of Science and Arts, Najran University, Najran-11001, Kingdom of Saudi Arabia.*
[3] *Promising Centre for Sensors and Electronic Devices (PCSED), Najran University, Najran-11001, Kingdom of Saudi Arabia.*
**Email:* schaudhary@pu.ac.in (S. Chaudhary), grc22@pu.ac.in (G.R. Chaudhary), ahmadumar786@gmail.com (Ahmad Umar)

CQDs derived from citric acid and ethylenediamine as starting precursors. Additionally, the fluorescence based solvatochromism can be tailored by adding electron-donating or electron-withdrawing groups over the surface of photoluminescent compounds.[48-50] Thus, the optical properties of CQDs can be modulated via surface modification. Sato *et al.*[48] reported the fluorescence solvatochromism in p-phenylenediamine-derived CQDs. The emission properties of formed CQDs were mainly aroused due to the alterations in the dipole interaction between solvent and formed CQDs surface. In spite of this, some accomplishment has been attained in facile fabrication of CQDs with broad solvatochromic shift range, especially the high quantum yield with better control over emission still has possessed serious confronts. In addition, the multistep fabrication strategies made the process more expensive and produced negative impact over the yield of CQDs. In this view, we have selected five different types of CQDs synthesized by calcination treatment of different fruit parts of *Aegle Marmelos* as a paradigm for analysing the systematic exploration of their optical and emission properties in ten different solvents of varying polarities. *Aegle marmelos* fruit was chosen as a role model to study the solvatochromic behaviour as different parts of fruit has different composition which result in different emission properties.[51-52] The excitation dependent emission behaviour in different solvents for five CQDs were examined to get insight into the emission centres in prepared CQDs. The emission behaviour of chosen CQDs was analyzed in detail to discuss the solvatochromic shift mechanisms in solvents of different polarities. The PL properties of chosen CQDs were also explored in a mixture of solvents with low and high polarities. The corresponding effect of different solvents on the emission centers of CQDs were thoroughly investigated by calculating the solvent $E_T(30)$ polarity parameter for all chosen solvents. To the best of our knowledge, the solvatochromic response of *Aegle marmelos* fruit derived carbon dots were studied for the first time. This work could unlock a new horizon to fabricate ratiometric probes of carbon dots for checking solvent polarity.

2. Experimental Section

2.1. Materials

Aegle Marmelos (Bael Patra) fruit was obtained from botanical garden, Panjab University for the synthesis of CQDs. Absolute ethanol of 99.9% purity was purchased from Changshu Yangyuan chemical, China. Different types of solvents namely: Cyclohexane, Chloroform, Toluene, Acetonitrile, Acetone, Propan-1-ol, DMSO and Methanol were purchased from Fisher Scientific with 99.9% purity. Aqua regia solution (HCL: HNO_3 = 3:1) was utilized to wash all the glass wares. The dialysis bag of molecular weight cut-off (MWCO) 1000 Da were used for the purification of particles. Quinine sulfate was procured from Sigma Aldrich with 99.9% purity. All the aqueous solutions were prepared in deionised water.

2.2. Instrumentation

An AICIL muffle furnace was used to carry out the thermal calcinations process. The ultra-centrifugation was done with REMI R-24 centrifuge. The absorption spectra of five different types of CQDs derived from *Aegle Marmelos* was evaluated using LABINDIA UV-Vis. spectrophotometer in the wavelength ranging between 200-800 nm. The photoluminescence properties of obtained CQDs were assessed using Perkin Elmer LS 55 PL spectrophotometer with excitation bandwidth 10 nm; emission bandwidth 10 nm; scan speed 200 nm/min respectively. The stirring and heating of sample was done using IKA C-MAG HS7 magnetic stirrer with ceramic heating plate. The nature of surface functionalised CQDs was assessed using Perkin Elmer (RX1) Fourier transform infrared (FT-IR) spectroscopy in the wavelength range from 4000-400 cm^{-1}. The elemental composition of CQDs was analysed by energy dispersive X-ray spectroscopy (EDX) with JEOL JSM 7500F FESEM instrument at 20 keV. The crystalline nature of CQDs was computed with Panalytical X'Pert Pro XRD diffractometer with a scanning rate of 2 deg. min^{-1} and monochromatic Cukα radiation in the 2θ scale 5-90°. The average crystalline size was calculated from the diffractogram peaks by using Debye Scherer formula,[53] *i.e.*

$$D=0.89\lambda/\beta Cos\theta \quad (1)$$

where D represents the mean crystallite size, λ is incident X-ray wavelength, β is full width at half maxima of diffraction peak which is represented in radians and θ is position of peak in the difractogram. Differential scanning calorimeter METTLER TOLEDO (Q20) instrument was used to explore the thermal properties of CQDs. The Thermogravimetric analysis (TGA-DTA) was performed with SDT Q-600 instrument. The hydrodynamic size and polydispersity index of developed CQDs was verified with MALVERN ZEN 1690 dynamic light scattering instrument. High resolution transmission electron microscopy (HRTEM) was accomplished on JEOL 2100F. Refractive index has been measured by Abbemat 500 automatic refractometer with precision value ± 2×10^{-5} and resolution of 1×10^{-6}.

2.3. Synthesis of C-dots from *Aegle Marmelos*

Aegle marmelos, an indigenous plant to India was used for the synthesis of CQDs. *Aegle marmelos* is one of the subtropical fruits of Rutaceae family.[54] The available bioactive compounds in different parts of *Aegle marmelos* have made it a highly useful plant with enormous medicinal worth. The antiamoebic and hypoglycaemic activities of fruits and roots of *Aegle marmelos* have made it effective material in Indian Ayurvedic system.[55] The antifungal, antidiabetic and anti-inflammatory activities of *Aegle marmelos* has enhanced its scope in curing human ailments. From different parts of bael tree, the medicinal and nutritional properties of fruits are believed to be more useful in Indian Ayurveda. Keeping in view the significance of bael tree in mind, the current study used the application of *Aegle Marmelos* as the starting

precursor for synthesising five different types of CQDs. Here, we have chosen different parts of bael fruit as they possess different chemical composition which results in different optical properties, activities and applications. The *Aegle Marmelos* -derived CQDs were fabricated as follows: Initially the bael fruit was cleaned by thorough washing with distilled water and then its covering, pulp, seed, gum and mixture of gum and pulp were separated to synthesize five different types of CQDs namely CQD_1 (from covering), CQD_2 (from pulp), CQD_3 (from seed), CQD_4 (from gum) and CQD_5 (from mixture of gum and pulp) respectively (Fig. 1). The covering, pulp, seeds and mixture of pulp and gum were chopped further and calcined at 250 °C in a muffle furnace for 90 min to completely remove the moisture content. The temperature was well optimised before subjecting the CQDs to calcination.[56] The bael gum was calcined at 350 °C in a muffle furnace for 180 min, as the texture of bael gum was thick and require higher temperature to yield finest carbon black. Heating at respective temperature result in degradation of polysaccharides, proteins and other components present in the fruit parts. The resultant residue of each part was homogeneously grinded into fine powder by using the electric mortar pestle. The solubility of five types of CQDs was checked in different solvents namely Cyclohexane, Chloroform, Toluene, Propanol, Acetone, Ethanol, Methanol, Acetonitrile, DMSO and water. All the five types of CQDs deciphers complete solubility in water and DMSO. The hydrodynamic size of CQDs obtained in case of different solvents was larger in contrast to water dispersed CQDs. Also, the quantum yield obtained in case of other solvents is comparatively lower as compared to water. It was well documented in the literature that water acts as the best solvent to perform dialysis for further purification of CQDs due to easy availability and low cost.[57] 2 gm of the resulting powder from each part suspended in 800 ml of water was magnetically stirred for 24 hr. The obtained solution was subjected to ultracentrifugation at 5000 rpm to remove any kind of impurity. The as-synthesised CQDs were further purified by using a dialysis bag with molecular weight cut-off (MWCO) 1000 Da.[58] The obtained purified CQDs displayed intense blue green fluorescence under UV illuminator (Fig. 1).

2.4. Quantum yield (ϕ) measurements

The respective values of quantum yield (ϕ) for *Aegle Marmelos* -derived CQDs from covering (CQD_1), pulp (CQD_2), seed (CQD_3), gum (CQD_4) and mixture of gum and pulp (CQD_5) were estimated by using Quinine sulfate dye as a reference standard material.[59] For the measurement, the aqueous solution of respective dye was made and ϕ was determined by using Equation 2.

$$\Phi = \Phi_r (I_x \mid I_r)(\eta_x^2 \mid \eta_r^2)(A_r \mid A_x) \quad (2)$$

where x denotes the CQDs, r is used for the standard dye, I is related to the fluorescence emission intensity of the respective system, A refers to the optical absorption values, η denotes the refractive index value of the material.

2.5. Effect of solvent polarity on the optical and fluorescence emission spectra of CQDs

The optical absorption and fluorescence emission behaviour of prepared CQDs were tested in presence of different solvents polarities ranging from low polarity solvents (such as cyclohexane, toluene, chloroform) to high polarity solvents (such as water, alcohols, DMSO). The sample preparation was done by taking 5 mg of dried CQDs into 10 ml glass vial. 5 ml of chosen solvent *i.e.* cyclohexane, toluene, chloroform, propanol, acetone, ethanol, methanol, acetonitrile, DMSO and water were added to the given dried CQDs sample. Each vial was thoroughly shaken and magnetically stirred for 1 h at 350

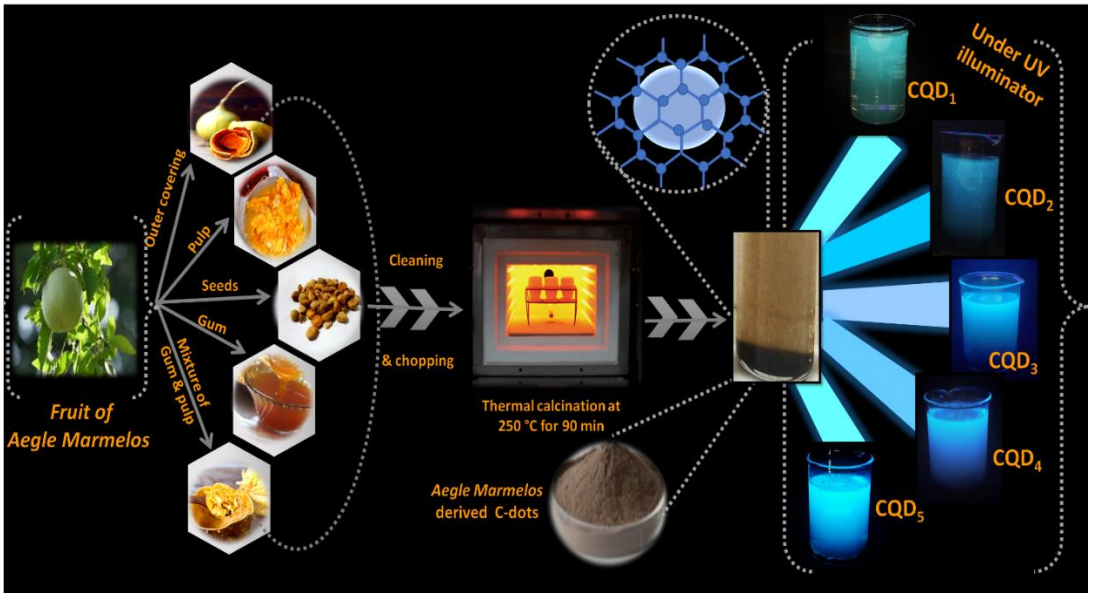

Fig. 1 Schematic representation showing the synthesis of *Aegle Marmelos* -derived CQDs from covering (CQD_1), pulp (CQD_2), seed (CQD_3), gum (CQD_4) and mixture of gum and pulp (CQD_5) respectively.

rpm to form solution. The excitation dependent studies were also performed in different solvents for investigating the emission behaviour. The solvent polarity (E_T30) and optical parameters of CQDs in different solvents were measured by taking the supernatant from each system.

3. Results and discussion

3.1 Structural and morphological studies of CQDs

The thermal calcination method has been used for the synthesis of five types of CQDs from the fruit of *Aegle Marmelos* (Fig. 1). The morphological characteristics of prepared CQDs were investigated by HRTEM analysis (Fig. 2ai to 2av). The prepared particles possess average particle size of 5 to 10 nm.[60] The crystalline lattice fringes and monodisperse nature of formed CQDs were clearly visible from the images.[61] The elementary composition of CQDs was analysed by energy dispersive X-ray spectroscopy (EDS) (Fig 2bi to 2bv). The existence of high carbon and oxygen contents in energy dispersive X-ray spectroscopic measurements suggest the existence of large number of hydroxyl, carbonyl and carboxyl groups on the surface of formed CQDs. Also, Table S1 shows the comparatively higher carbon content which clearly signifies successful synthesis of CQDs. In addition, 3.97% to 5.89% of nitrogen content was also found in CQD_2 to CQD_5. However, the presence of nitrogen was absent in case of CQD_1 (Table S1). Fig. S1 shows that hydrodynamic diameters of prepared CQDs with PDI value of 0.422, 0.463, 0.443, 0.451 and 0.50 for CQD_1 to CQD_5.

The X-Ray diffraction (XRD) patterns of *Aegle Marmelos*-derived CQDs were used to determine the phase structure and size of prepared particles. For instance, CQD_1 displayed an intense diffraction peak at 23.8° which belongs to the (002) plane (Fig. 3a). This was related to the interlayer packing of disordered carbon leading to the formation of turbostratic structure in CQDs.[62-63] The crystallite size was found to be 1.179 nm by using Debye Scherer equation. In addition, the broad peak was due to the amorphous nature of formed particles. The additional weak peak at 40° indicates a certain degree of graphitization in CQD_1 sample. The XRD spectra of CQD_2 shown an intense sharp peak at 21.1°and a weak peak at 34.79° for (002) and (100) plane of graphitic carbon respectively (Fig. 3b). The calculated interlayer distance (d-spacing) was 1.035 nm for (002) plane. The XRD profile of CQD_3 shown the existence of two intense sharp peaks at 20.6°C and 30.3° C for (002) and (100) planes of graphitic carbon. The interlayer distance for CQD_3 was approximately 1.48 nm and 3.52 nm for the (002) and (100) planes respectively (Fig. 3c). An intense sharp peak at $2\theta = 24.7°$ and weak broad peak appeared at $2\theta = 40.9°$ was observed for CQD_4 particles (Fig. 3d). The calculated d-spacing was 1.39 nm for (002) plane of CQD_4.[64]

The XRD spectrum of CQD_5 shown a sharp peak at 20.9° which belonged to (002) plane of graphitic carbon (Fig. 3e). The average crystallite size was found to be 1.62 nm for CQD_5. The data was found to be comparable with the HRTEM results.

FTIR spectra of CQDs indicates the existence of numerous types of hydrophilic functional groups like –COOH, -N-H, -OH on their surface which is further correlated to their excellent solubility in water.[65-66] The peak observed at 3293cm^{-1} belongs to C–OH stretching vibration in CQD_1 (Fig. 3a). The peak at 2980 cm^{-1} was due to the C–H stretching vibrations. The bending vibrations of N–H appear at 1391 cm^{-1}. The peak appearing at 1565 cm^{-1} and 1069 cm^{-1} indicates the presence of C═O and C–O stretching vibrations respectively (Fig. 3a).

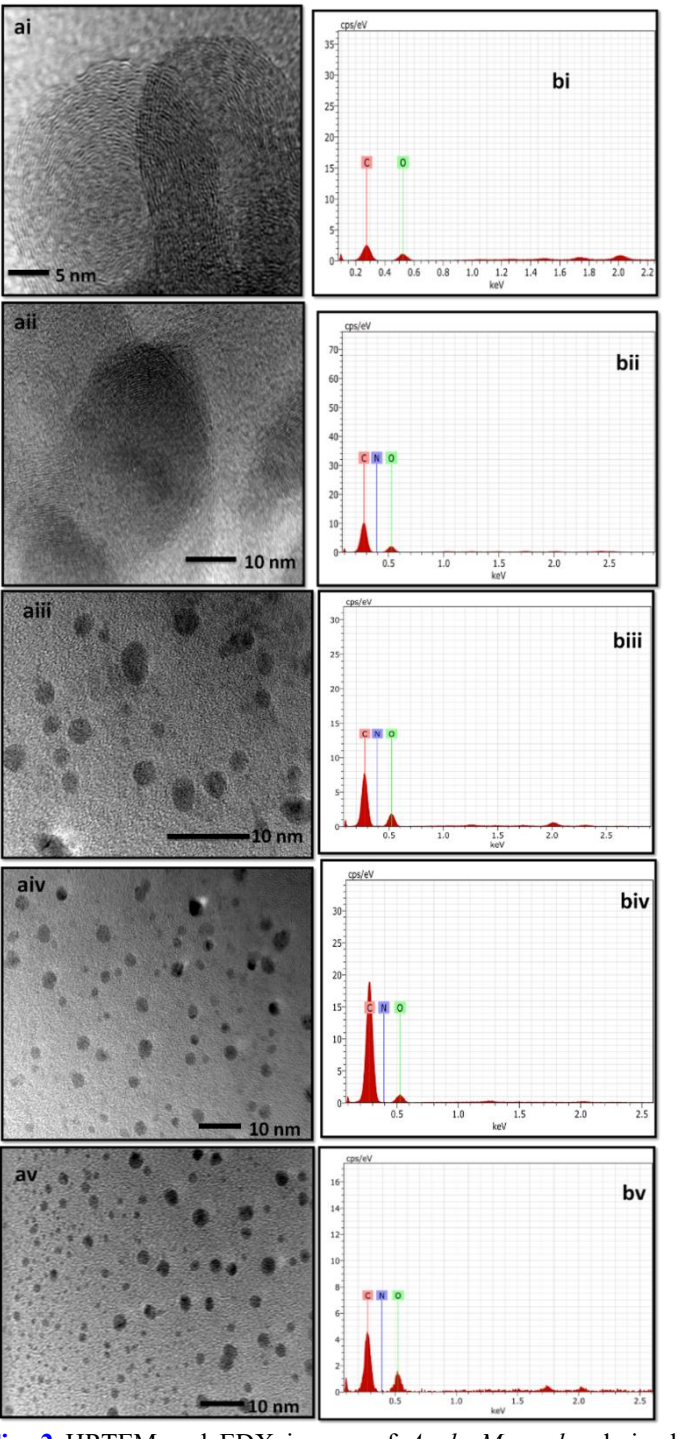

Fig. 2 HRTEM and EDX images of *Aegle Marmelos*-derived CQD_1 (ai, bi), CQD_2 (aii, bii), CQD_3 (aiii, biii), CQD_4 (aiv, biv) and CQD_5 (av, bv) respectively.

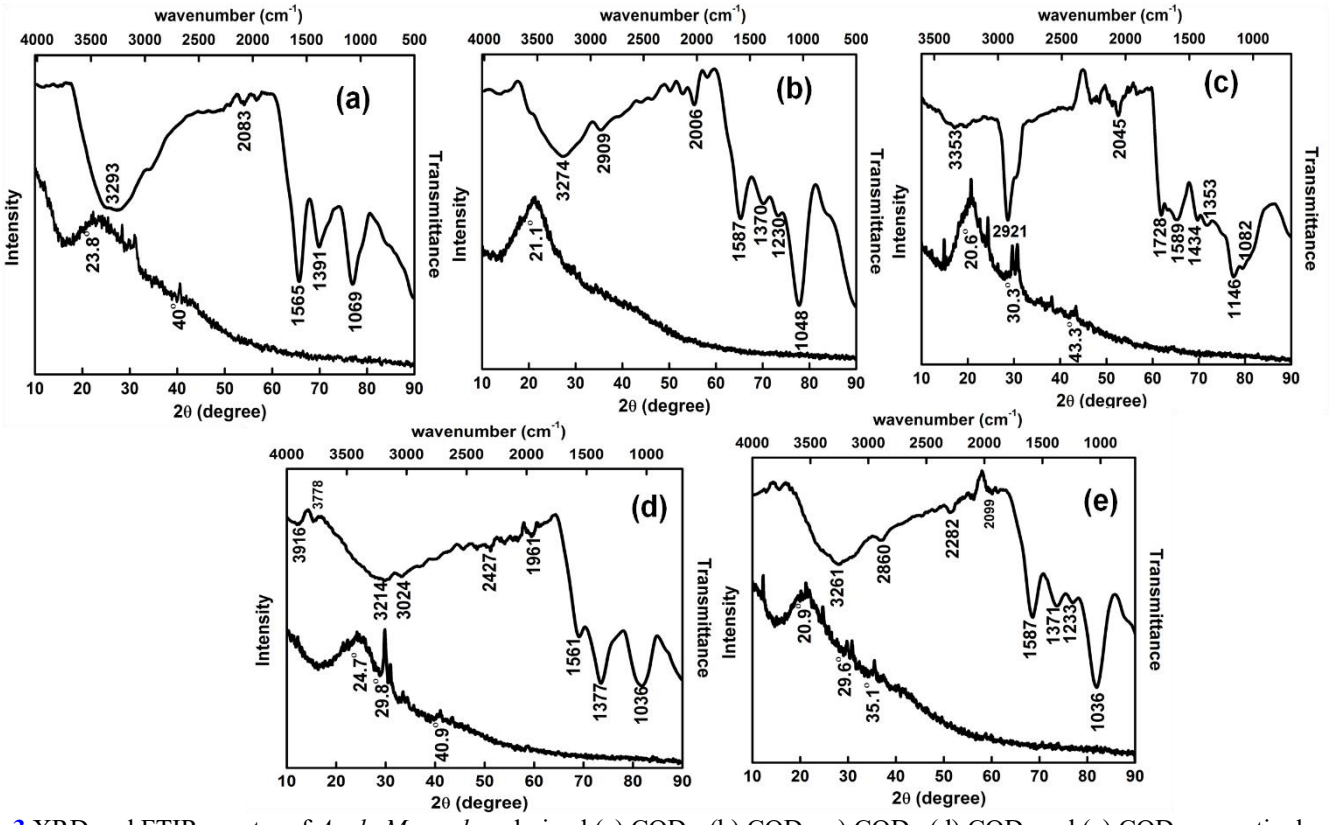

Fig. 3 XRD and FTIR spectra of *Aegle Marmelos* -derived (a) CQD_1, (b) CQD_2, (c) CQD_3, (d) CQD_4 and (e) CQD_5 respectively.

The FTIR spectra of CQD_2 showed a broad –OH stretching peak at 3274 cm^{-1}. The C–H stretching peak was observed at 2909 cm^{-1} and the peak at 1587 cm^{-1} indicates the existence of C═O group (Fig. 3b). Further the peak observed at 1370 cm^{-1} represents the N–H group. The peak appearing at 1048cm^{-1} belongs to C–O stretching vibration (Fig. 3b). A broad peak appearing between 3450 cm^{-1} and 3100 cm^{-1} corresponds to –OH stretching vibrations in CQD_3. The sharp peak at 2921 cm^{-1} depicts the C–H stretching and hump appearing at 1728 cm^{-1} is due to C═O group vibrations. The bending vibration of N–H appears at 1434 cm^{-1}. Moreover, the peak at 1082 cm^{-1} result from C–O stretching vibration (Fig. 3c). The FTIR spectra of CQD_4 showed a broad peak at 3214 cm^{-1} due to the –OH stretching vibration. A broad band at 3024 cm^{-1} is attributed to C–H bond stretching vibrations in CQD_4 (Fig. 3d). A sharp and intense peak at 1036 cm^{-1} shows the occurrence of C–O stretching vibrations whereas a weak peak observed at 1561 cm^{-1} corresponds to C=O stretching vibration. The N–H stretching vibration emerged at 1377 cm^{-1} in case of CQD_4 (Fig. 3d). A broad band observed at 3261cm^{-1} shows the –OH stretching vibration with a C–H stretching vibration shoulder at 2890 cm^{-1} for CQD_5 (Fig 3e). The bending vibration for N–H appears at 1371 cm^{-1}. The peaks appearing at 1587 cm^{-1} and 1036 cm^{-1} indicate the existence of C═O and C–O stretching vibrations in CQD_5 (Fig. 3e). The comparison of FTIR spectrum for all the five prepared CQDs result in two major observations. One is the stretching vibrations of both C=O and C-O were found to be very sharp and discrete in CQD_1, CQD_2, and CQD_5 (Fig. 3). However, the peaks were integrated in case of CQD_3 and CQD_4 which lead to increased degree of oxidation in CQDs prepared from seeds and gum of *Aegle Marmelos*. The second observation shows that the -OH stretching vibration was enhanced in CQD_1 and CQD_5 as compared to other three samples. The enhanced and broad –OH peak specifies the existence of more hydroxyl groups on the CQDs surface which result in high polarity and dispersibilty of CQD_1, CQD_5 as compared with CQD_2, CQD_3 and CQD_4. For getting the information about the thermal stability of prepared CQDs in different temperature ranges, the respective particles were subjected to TGA measurement in temperature range of 0-1000 °C (Fig. S2). In case of CQD_1, the first 5% weight loss between 30 °C to 120 °C aroused due to loss of water molecules associated with particles. The second weight loss of 35% between 300 °C to 600 °C was due to the loss of different functional groups attached on the surface of CQD_1. It was clearly represented by the DTG peak at 340°C in Fig. S2a. However, a distinct mass loss of 6% in temperature range of 30-110 °C and 20 °C to 90 °C was observed in case of CQD_2 and CQD_3 (Fig. S2b and Fig. S2c). An additional weight loss of 47% and 40% between 250 °C to 550 °C and 300 °C to 470 °C may be attributed to the loss of surface functional groups in CQD_2 and CQD_3 with DTG peak at 336 °C and 385 °C. After 650 °C, there was no significant weight loss observed in case of CQD_2 and CQD_3. TGA spectra for CQD_4 showed the first weight loss of 15%, between 15 °C to 150 °C and second weight loss of 20% between 460 °C to 800 °C. However, CQD_5 displayed the first weight loss of 10% between 20 °C to 105 °C. The second weight loss of 47%

between 250 °C to 550 °C is due the condensation of different functional groups presents on the surface of CQDs. The DTG curve clearly indicates the weight loss peak at 335 °C for CQD_5 (Fig. S2e). The differential scanning calorimeter analysis of CQDs was done in order to study the thermal behaviour of prepared CQDs. The single endothermic peak with transition temperature of 355.9 °C was observed for CQD_1, CQD_4 and CQD_5 (Fig. S2f). The transition temperature comes out to be 358.06 °C for CQD_2 and CQD_3 with endothermic peak.

3.2 Optical and emission properties of CQDs

The aqueous solution of all the prepared CQDs in absorption spectra has displayed two significant peaks. The absorption peak at 262 nm, 282 nm, 290 nm, 258 nm, 266 nm arise from the "core state" of CQD_1, CQD_2, CQD_3, CQD_4 and CQD_5 respectively. These peaks were mainly aroused due to the $\pi - \pi^*$ transitions in graphene like core of prepared CQDs. The second absorption peak at 364 nm, 367 nm, 351 nm, 361 nm and 373 nm for CQD_1, to CQD_5 were due to the occurrence of functional groups on the edge of the core (Fig. 4).[67] This will further assist the transfer of negatively charged ions from the non-bonding orbital of heteroatom to the π^* orbital of the core leading to $n-\pi^*$ transitions in prepared CQDs. In addition, these absorption transitions from core and edge state give rise to hole-electron excitons in formed CQDs in aqueous media. Moreover, the outcomes have pointed towards the susceptibility of the precursor material for the optical properties of the as synthesized CQDs.

The outcomes were further verified by performing the fluorescence emission studies as function of excitation wavelength in range of 270 nm to 340 nm for all the five types of formed CQDs. The water dispersed CQD_1 samples have shown maximum emission peak at 430 nm via exciting the samples at 320 nm. CQD_2 and CQD_3 samples have displayed maximum emission peak at 430 nm and 440 nm via exciting the samples at 340 nm respectively. The maximum emission peak for CQD_4 and CQD_5 were observed at 430 nm by exciting the samples at 330 nm. These outcomes are mainly related to the existence of surface related defective sites on prepared CQDs. The respective values of the Stokes shift obtained from the emission spectra for maximum emission peak of five different types of CQDs with reference to the absorption peak is around 168 nm, 148 nm, 150 nm, 172nm and 164 nm for CQD_1 to CQD_5. The behavioural changes in the values of Stokes shift was correlated with the nature of surface state on prepared CQDs. These surface states will further affect the electronic transitions in formed particles. The tapering of emission peaks in CQD_1 and CQD_3 were due to the higher surface oxidation rate in these particles as compared to CQDs formed from pulp, gum and mixture of pulp and gum. The Gaussian studies for the highest emission intensity peak for CQD_1 was done to get information about the defect states in formed particles (Fig. 4b inset). The splitting of broad emission peak into three sub peaks was due to the existence of defect-charged excitons, defect-bound excitons and electron

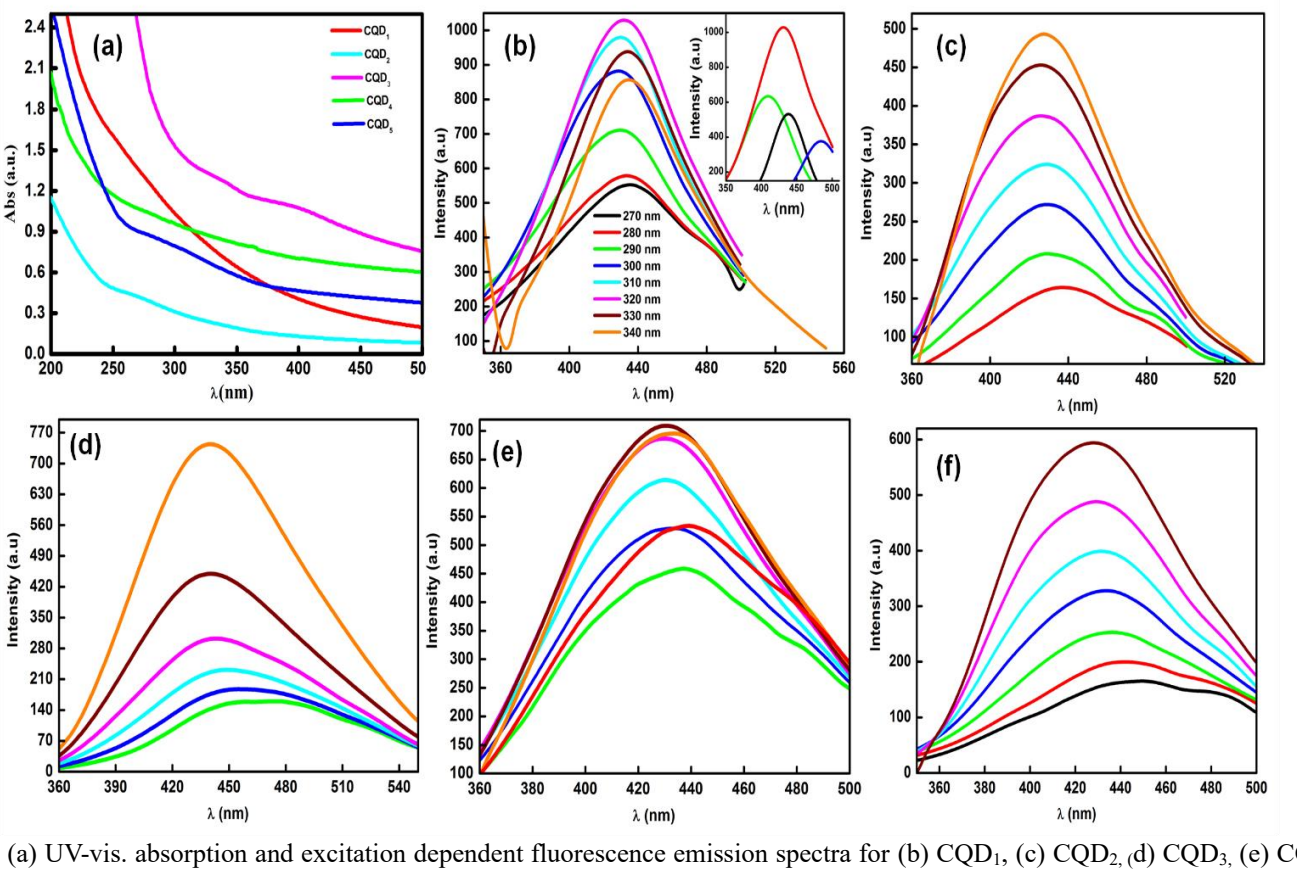

Fig. 4 (a) UV-vis. absorption and excitation dependent fluorescence emission spectra for (b) CQD_1, (c) CQD_2, (d) CQD_3, (e) CQD_4 and (f) CQD_5.

hole recombination effect in CQDs[68] The respective peak positions with area under the curve values and full width at half maxima values for all the CQDs were given in Table S2 (supplementary data).

3.3 Effect of different solvents on the Optical and emission properties of CQDs

The corresponding effect of ten different solvents including cyclohexane, toluene, chloroform, propanol, acetone, ethanol, methanol, acetonitrile, DMSO and water was studied on the optical behaviour of different types of CQDs prepared from the different parts of *Aegle Marmelos* fruit. The choice of the solvent was based on the polarity parameters which cover the broad range of solvent polarity and hydrogen bonding with the CQDs (Table S3). There was no obvious peak below 240 nm for all the prepared CQDs in UV-vis. spectra (Fig. S3). However, absorption humps were observed between 260nm to 350 nm in case of chosen solvents for model CQDs. For instance, the absorption spectra of CQD_1 (toluene, cyclohexane, acetone, methanol, chloroform, acetonitrile, propanol, ethanol, water and DMSO) displayed a distinct absorption hump at 270, 272, 273, 275, 284, 313, 315, 320 and 324 nm. These absorption humps were aroused due to the π-π^* transition in the graphitic core and n-π^* transition of carboxyl, hydroxyl and amino groups present over the edge of CQDs. In addition, the shift in absorption peak in different solvents were attributed to the reduced bandgap between HOMO and LUMO in CQDs. Similar, solvent dependent variations were observed in case of other CQDs. The behaviour changes were comparable with most of the solvatochromic dyes.[69] All five types of CQDs render magnificent solubility in presence of propanol, ethanol, DMSO and water as compared to other polar solvents like methanol and acetonitrile. However, relatively poor dispersibilty was observed in presence of toluene as compared with other non-polar solvents like cyclohexane, chloroform. The precipitation of CQDs was also appeared in this solution after 2-3 hr. Fig. S4 shows that the position of emission peak is not linearly dependent on dielectric constant. This was mainly due to the dependency of the ground and excited state of the CQDs over the surrounding environment provided by the chosen solvent. Moreover, all the five types of CQDs have also displayed excitation dependent (280 nm to 340 nm) emission behaviour irrespective of the nature of solvent (Fig. S5).

Considering the excitation wavelength of each CQDs solution (dispersed in water) at which it shows maximum intensity, has been further used to study the solvatochromic response of CQDs. The shift in the emission wavelength of different types of CQDs shows difference in presence of same solvents. Here it confirms that the asynthesised five types of CQDs differs in their chemical composition. The outcomes are statistically significant and supported the solvatochromism effect in prepared CQDs. The formation of multiple peaks in CQD_3 in presence of propanol and acetonitrile at λ_{ex} = 280 nm and in presence of chloroform at λ_{ex} = 340 nm was associated with the formation of cross-linked structures in π conjugated

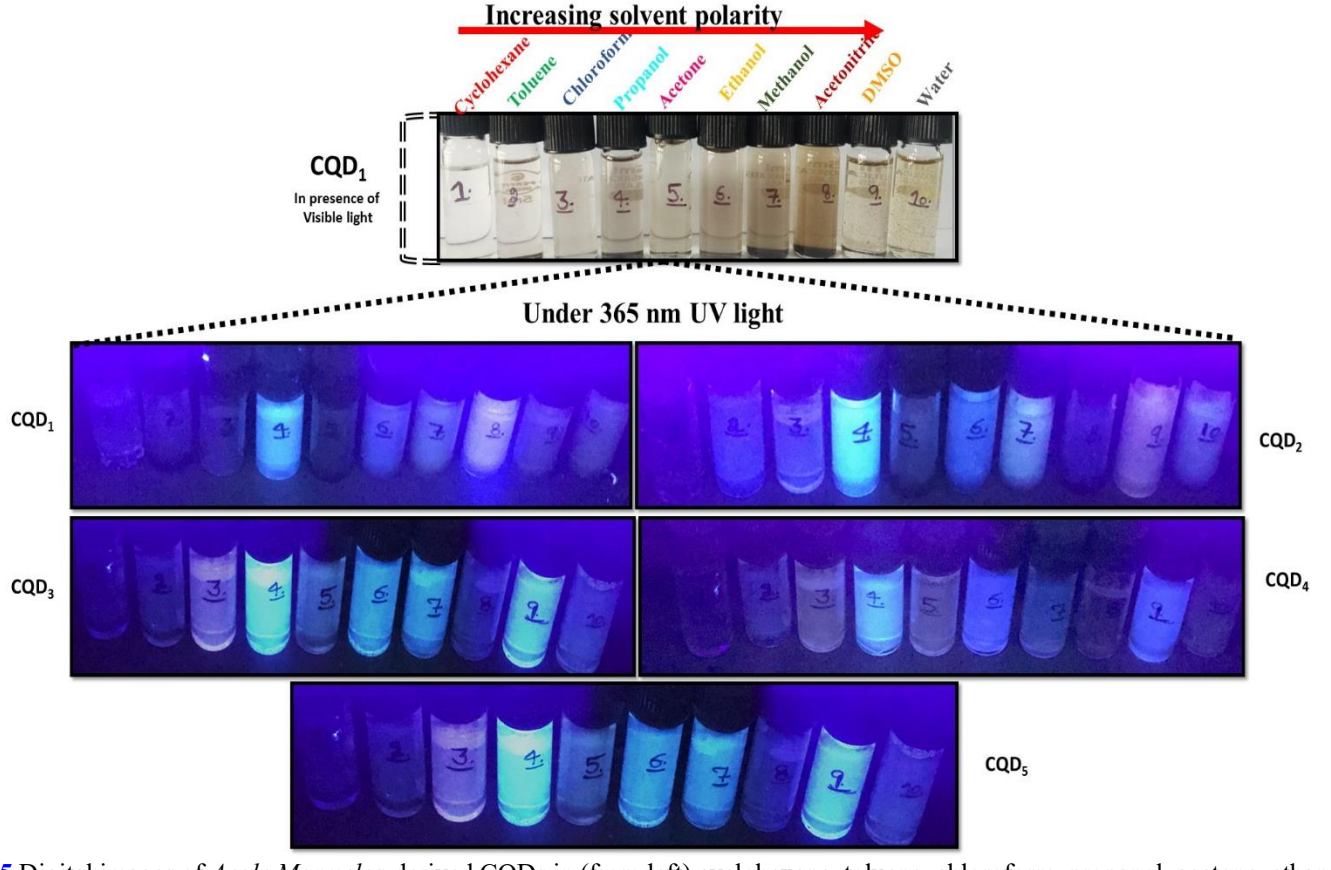

Fig. 5 Digital images of *Aegle Marmelos*-derived CQDs in (from left) cyclohexane, toluene, chloroform, propanol, acetone, ethanol, methanol, acetonitrile, DMSO and water under visible light (only for CQD_1) and 365 nm UV light (for all five types).

system (Fig. S5c). The digital photographs of prepared CQD_1 dispersion in ten different solvents under white light was shown in Fig. 5. The resulting photoluminescence spectra for all the prepared CQDs have displayed solvent dependent shift at same excitation wavelength (Fig. 6). The light brown color dispersion of CQD_1 was observed in case of propanol, acetone, and ethanol. However, the darker coloration of CQD_1 was observed in presence of methanol and acetonitrile solvent. The clear yellowish suspension of CQD_1 was observed in presence of DMSO and water.[70] These changes in the color were aroused due to the differences in the light absorption properties of CQD_1 in presence of different solvents. Similar changes were observed for other CQDs. Fig. 5 shows that the CQD_1 are poorly soluble in cyclohexane, toluene, chloroform, partially soluble in propanol, acetone, ethanol and soluble in methanol, acetonitrile along with some precipitate settled at the bottom. Whereas CQD_1 renders complete solubility in DMSO and water. Similar solubility outcomes were obtained from CQD_2 to CQD_5. However, digital images of CQDs in ten different solvents under 365 nm UV light are shown in Fig. 5. The prepared CQDs dispersions displayed light yellowish emission in presence of chloroform and acetone, under UV light. However, bluish emission was observed for all types of CQDs except CQD_2 in presence of propanol, ethanol and DMSO, respectively. CQD_2 displayed orange-yellow emission in presence of DMSO. In addition, blue emission intensities of all types of CQDs were found to be maximum in presence of propanol. These observable changes are due to the surface modification and solvent dependent solvatochromism in prepared CQDs.

On interpreting the effect of solvent on the emission spectra of prepared CQDs in different solvents, it was observed that the peak displayed red shifts in emission spectra with increasing the polarity of chosen solvent (Fig. 6). This behavioural aspect was aroused due to the solvation effect, which further reduced the HOMO and LUMO band gap energy with increasing the polarity of the solvents. In addition, the shift in the peaks was associated with the non-uniformity of the existing π conjugated structures in CQDs. The position of the peak in CQD_1 has been red shifted by 47 nm on changing the solvent from cyclohexane to water. The higher red shift in peak positions was mainly associated with the higher value of dipole interaction and increasing rate of hydrogen bonding interactions between the solvent and surface of CQDs in presence of polar solvents. However, the shift of 2 nm and 29 nm was observed for changing the solvent from cyclohexane to Toluene and chloroform respectively (Fig. 6a). Similar variations were observed for other types of prepared CQDs. This behavioural change in peak position towards the right is mainly aroused due to the affirmative solvatochromism in fluorescence. However, the increase in solvent polarity (E_T30) has produced a decreasing effect on the emissive energy of each type of CQDs (Fig. 7). The outcomes have clearly supported the effect of solvent polarity on the fluorescence solvatochromism. The results of CQD_1, CQD_2, CQD_3, CQD_4 and CQD_5 exhibited almost similar linear relationship. The emission energy of CQD_4 at given E_T value was found to be higher than other four CQDs. The corresponding effect of different CQDs in presence of different solvents has also been visualized by measuring the

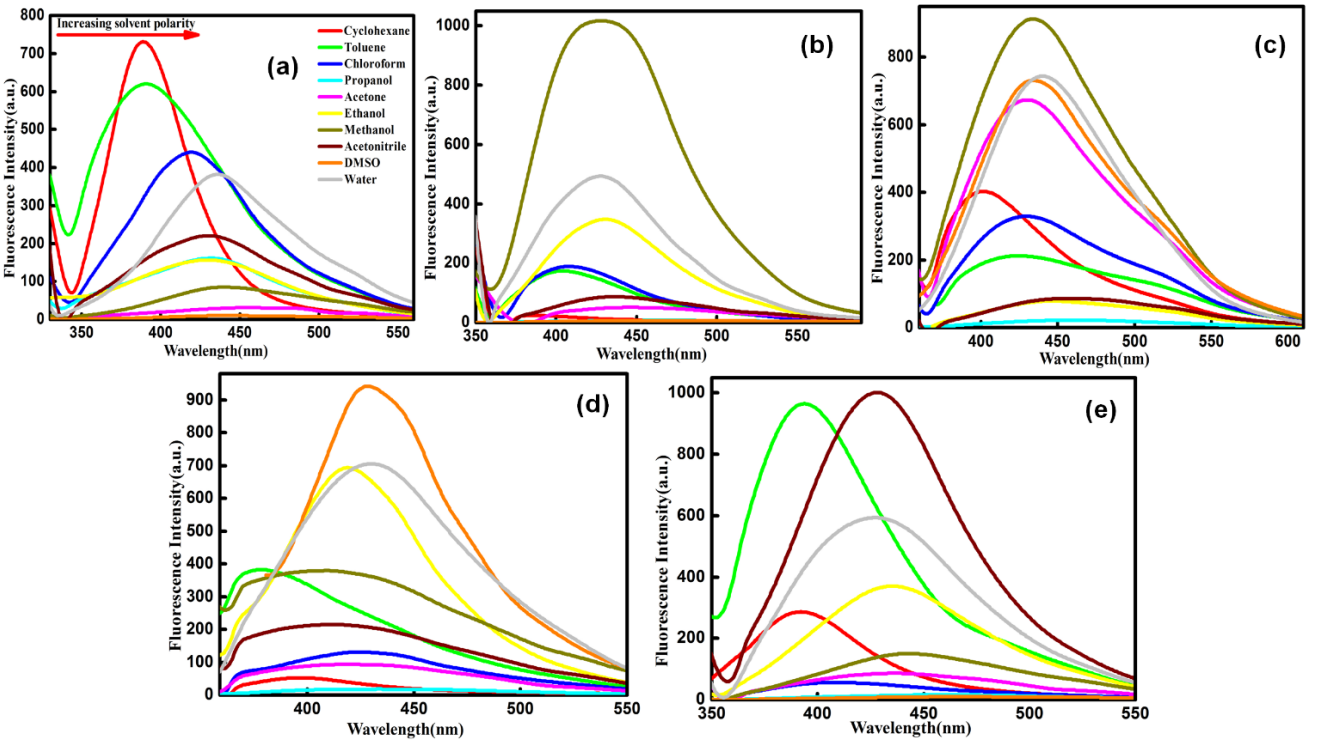

Fig. 6 Fluorescence emission spectra of *Aegle Marmelos* -derived (A) CQD_1, (B) CQD_2, (C) CQD_3, (D) CQD_4 and (E) CQD_5 in presence of cyclohexane, toluene, chloroform, propanol, acetone, ethanol, methanol, acetonitrile, DMSO and water.

effect on refractive index. The existence of different functional moieties on the exterior surface of CQDs has made them dispersible in different organic solvents. However, the good dispersibilty of CQDs was found in aqueous solutions. Thus, the effect of formed CQDs was investigated by measuring the refractive index by using the Equation (3)

$$\text{Refractive index (n)} = c/V \quad (3)$$

where c is the velocity of light in vacuum and V is velocity of light in medium. Also,

$$V = f\times\lambda \quad (4)$$

$$n = c/f\lambda \quad (5)$$

where f is the frequency of the wave and λ is the wavelength of the wave. The obtained refractive index values of all types of CQDs were listed in Table S4. On interpreting the results, it was found that the presence of CQDs in solvent has reduced the original value of refractive index. This may be attributed to the increase in the velocity of light in medium *i.e.* V, which in turn is dependent on the wavelength and frequency of the wave. In presence of CQDs, the wavelength of solvent increased thereby enhanced the velocity of light in medium and hence reduced the value of refractive index. Fig. S6 presented a plot of maximum emission peak value (in eV) with refractive index of various solvent. The emission peak value for all the prepared CQDs followed similar trend with refractive index values of solvents. In addition, the refractive index values vary inversely with the polarity of solvent *i.e.* as we move towards most polar solvent (water), the respective refractive index value decreases for all the samples.

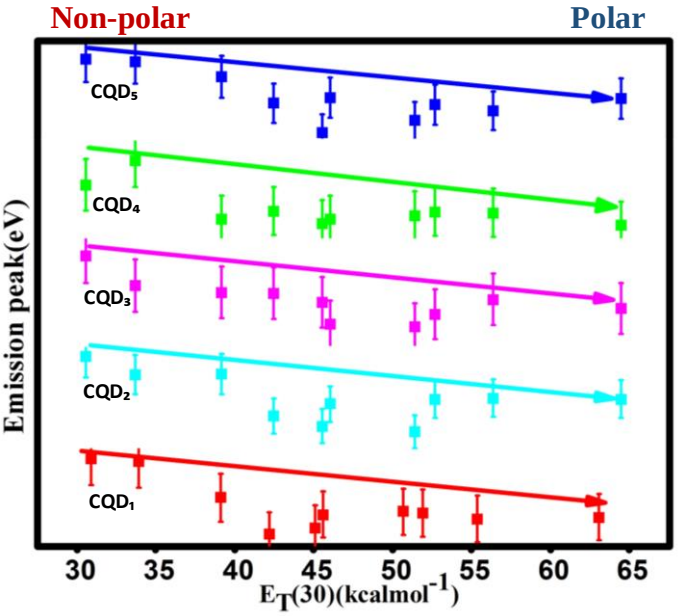

Fig. 7 Relationship between solvent polarity parameter (E_T30) and maximum emission wavelength (in eV) of *Aegle Marmelos* - derived CQDs.

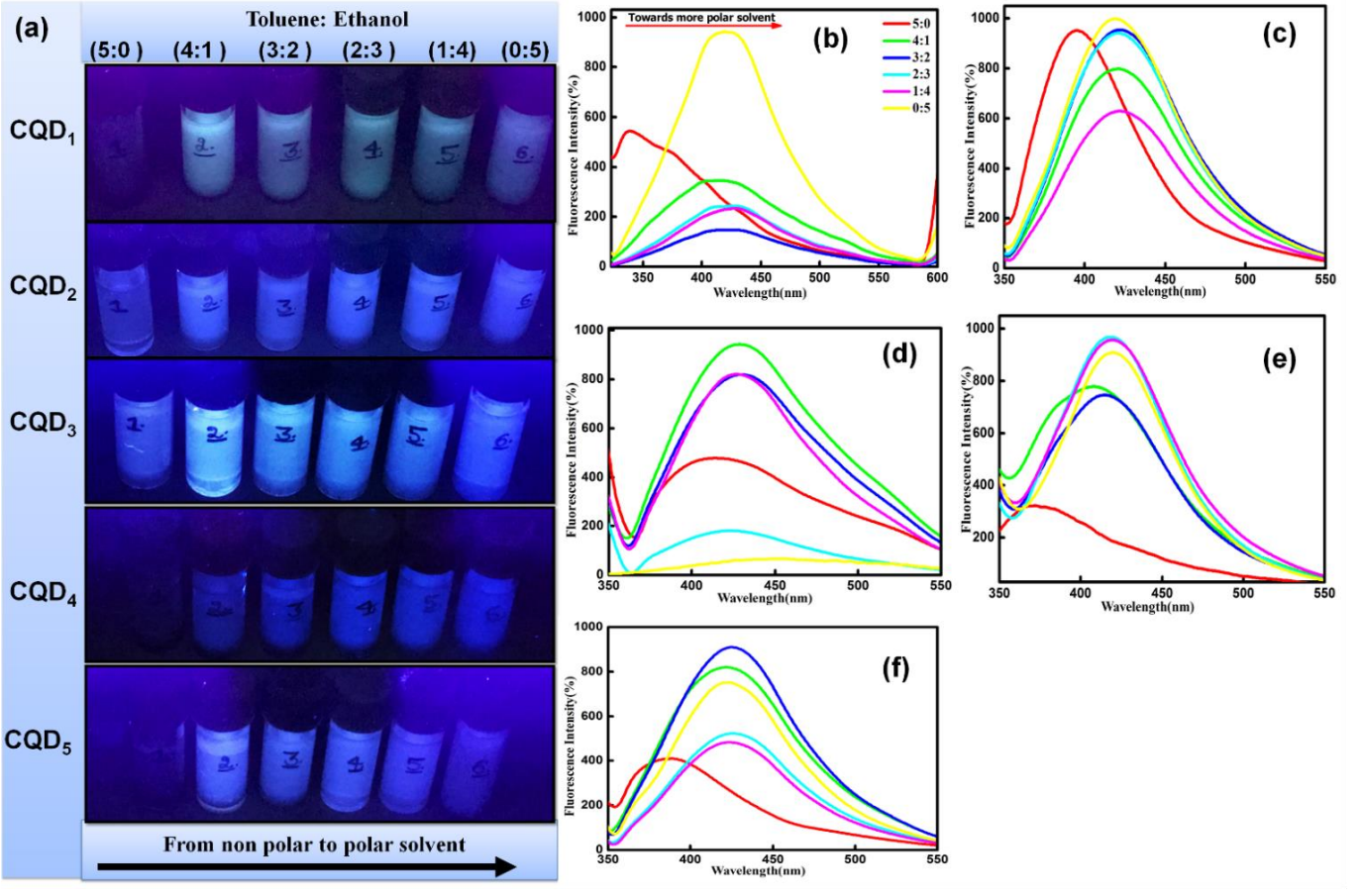

Fig. 8 (a) Digital images in presence of 365 nm UV light and PL spectra of (b) CQD_1, (c) CQD_2, (d) CQD_3, (e) CQD_4 and (f) CQD_5 in mixture of toluene and ethanol. From left the dilution factors are 5:0, 4:1, 3:2, 2:3, 1:4 and 0:5 respectively.

3.4 Effect of mixture of solvent with high and low polarity on emission properties of CQDs

We have further investigated the photoluminescence property of CQDs in a mixture of solvents with low and high polarities (*i.e.* different ratio of toluene and ethanol). Fig. 8a shows the digital images of dispersions in mixture with different ratios of toluene and ethanol under UV light. The emission spectra of all CQDs excited with optimum wavelengths was plotted in Fig. 8b to 8f. The spectra displayed significant red shift of 77 nm in emission peak with increase in the ratio of ethanol in the solvent mixture for CQD_1. However, the shift of 25, 38, 49 and 40 nm was observed for CQD_2, CQD_3, CQD_4 and CQD_5 in emission peak with increase in the ratio of ethanol in the solvent mixture. The outcomes have clearly depicted the proportionality ratio of high and low polarity solvents for CQDs.

4. Conclusion

The current work represented the formation of five different types of CQDs from the different fruit parts of *Aegle Marmelos.* The formed particles have displayed high solubility and low toxicity. The respective values of the Stokes shift in the emission spectra for maximum emission peak for the five different types of CQDs corresponding to the absorption peak is about 168 nm, 148 nm, 150nm, 172nm and 164 nm for CQD_1 to CQD_5. The particles have displayed polarity-dependent absorption and emission behaviour in ten different solvents. The dispersion of formed CQDs in ten different solvents varied on the basis of polarities has displayed the changes in the color from light blue to orange-yellow to red with enhancing the polarity of the solvent. Among the synthesised CQDs, CQD_1 exhibits longest emission wavelength range from 389 nm to 436 nm from non-polar to polar medium. This fluorescence behaviour of carbon dots has been assigned to the increasing tendency of CQDs to form hydrogen bonding with different solvents. Additionally, CQDs exhibits linear relationship between emission wavelength and proportion ratio of ethanol in mixture of high polarity and low polarity solvents. CQDs prepared in this work have displayed a higher blue intensity of light; therefore, it is expected to play a significant role in color changing layers for LEDs.

Acknowledgment

Anjali Vijeata is thankful to Council of Scientific and Industrial Research (CSIR), New Delhi for financial support under CSIR (09/135(0894)/2019-EMR-l). Savita Chaudhary is thankful to DST Inspire Faculty award [IFACH- 17], Haryana State Council for Science and Technology [HSCSIT/R&D/2020/476], DST Chandigarh and DST Purse grants II for financial assistance. Ganga Ram Chaudhary would like to acknowledge the support of UGC, India under the INDO-US 21st Century knowledge Initiative project [F.No. 194-2/2016 (IC)]. The authors are thankful to the Sophisticated Analytical Instrumentation Facility (SAIF, CIL), Panjab University, Chandigarh. Authors are thankful to Panjab University SAIF CIL for technical support. Ahmad Umar would like to acknowledge Najran University for the support.

Supporting information

Supplementary data to this file can be found online.

Conflict of interest

There are no conflicts to declare.

References

[1] P. Das, S. K. Bhattacharyya, P. Banerji, N. C. Das, *Nano-Struct. Nano-Objects.*, 2021, **25**, 100641, doi: 10.1016/j.nanoso.2020.100641.

[2] S. Zhu, Q. Meng, L. Wang, J. Zhang, Y. Song, H. Jin, K. Zhang, H. Sun, H. Wang, B. Yang, *Angew. Chem., Int. Ed.*, 2013, **52**, 3953–3957, doi: 10.1002/anie.201300519.

[3] F. H. Horst, C. V. S. Rodrigues, P. H. P. R. Carvalho, A. M. Leite, R. B. Azevedo, B. A. D. Neto, J. R. Corrêa, M. P. Garcia, S. Alotaibi, M. Henini, S. B. Chaves, M. O. Rodrigues, *RSC Adv.*, 2021, **11**, 6346-6352, doi: 10.1039/D0RA10859F.

[4] C. Li, X. Sun, Y. Li, H. Liu, B. Long, D. Xie, J. Chen, K. Wang, *ACS Omega*, 2021, **6**, 3232–3237, doi: 10.1021/acsomega.0c05682.

[5] Z. Yi, X. Li, H. Zhang, X. Ji, W. Sun, Y. Yu, Y. Liu, J. Huang, Z. Sarshar, M. Sain, *Talanta*, 2021, **222**, 121663, doi: 10.1016/j.talanta.2020.121663.

[6] A. Tan, G. Yang, X. Wan, *Spectrochim. Acta Part A*, 2021, **253**, 119583, doi: 10.1016/j.saa.2021.119583.

[7] Y. Jiang, X. Zhang, L. Xiao, R. Yan, J. Xin, C. Yin, Y. Jia, Y. Zhao, C. Xiao, Z. Zhang, W. Song, *Carbon*, 2020, **163**, 26-33, doi: 10.1016/j.carbon.2020.03.013.

[8]O.T. Bruns, T. S. Bischof, D. K. Harris, D. Franke, Y. Shi, L. Riedemann, A. Bartelt, F. B. Jaworski, J. A. Carr, C. J. Rowlands, M. W. B. Wilson, O. Chen, H. Wei, G. W. Hwang, D. M. Montana, I. Coropceanu, O. B. Achorn, J. Kloepper, J. Heeren, P. T. C. So, D. Fukumura, K. F. Jensen, R. K. Jain, M. G. Bawendi, *Nat. Biomed. Eng.*, 2017, **1**, 56, doi: 10.1038/s41551-017-0056

[9] Y. Wang, Q. Zhang, J. Gong, X. Zhang, *Dyes Pigments*, 2021, **189**, 109261, doi: 10.1016/j.dyepig.2021.109261.

[10] S. Delavari, S. Ziadzade, J. K. Rad, V. Hamrang, A.R. Mahdavian, *Carbohydr. Polym.*, 2020, **247**, 116756, doi: 10.1016/j.carbpol.2020.116756.

[11] B. Yotnoi, M. Sinchow, A. Ngamjarurojana, A. Rujiwatra, *Inorg. Chim. Acta*, 2020, **500**, 119236, doi: 10.1016/j.ica.2019.119236.

[12] E. Gharibshahi, *Solid State Commun.*, 2020, **320**, 114009, doi: 10.1016/j.ssc.2020.114009.

[13] X. Huang, B. Cui, Y. Ma, X. Yan, L. Xia, N. Zhou, M. Wang, L. He, Z. Zhang, *Anal. Chim. Acta*, 2019, 1078, 125-134, doi: 10.1016/j.aca.2019.06.009.

[14] Y. Hu, Y. Wang, C. Wang, Y. Ye, H. Zhao, J. Li, X. Lu, C. Mao, S. Chen, J. Mao, L. Wang, Q. Xue, *Carbon*, 2019, **152**, 511-520, doi: 10.1016/j.carbon.2019.06.047.

[15] H. Wang, M. Zhang, Y. Song, H. Li, H. Huang, M. Shao, Y.

Liu, Z. Kang, *Carbon*, 2018, **136**, 94-102, doi: 10.1016/j.carbon.2018.04.051.
[16] T. Boobalan, M. Sethupathi, N. Sengottuvelan, P. Kumar, P. Balaji, B. Gulyás, P. Padmanabhan, S. T. Selvan, A. Arun, *ACS Appl. Nano Mater.*, 2020, **3**, 5910–5919, doi: 10.1021/acsanm.0c01058.
[17] S. R. Ankireddy, V. G. Vo, S. S. An, A. J. Kim, *ACS Appl. Bio Mater.*, 2020, **3**, 4873–4882, doi: 10.1021/acsabm.0c00377.
[18] K.M. Omer, D.I. Tofiq, A.Q. Hassan, *Microchim. Acta*, 2018, **185**, 466, doi: 10.1007/s00604-018-3002-4.
[19] P. D. Khavlyuk, E. A. Stepanidenko, D. P. Bondarenko, D. V. Danilov, A. V. Koroleva, A. V. Baranov, V. G. Maslov, P. Kasak, A. V. Fedorov, E. V. Ushakova, A. L. Rogach, *Nanoscale*, 2021, **13**, 3070-3078, doi: 10.1039/D0NR07852B.
[20] D. Li, J. Huang, R. Li, P. Chen, D. Chen, M. Cai, H. Liu, Y. Feng, W. Lv, G. Liu, *J. Hazard Mater.*, 2021, **401**, 123257, doi: 10.1016/j.jhazmat.2020.123257.
[21] Y. Tu, S. Wang, X. Yuan, Y. Xiang, K. Qin, Y. Wei, Q. Zhang, X. Chen, X. Ji, *Dyes Pigments*, 2021, **184**, 108761, doi: 10.1016/j.dyepig.2020.108761.
[22] P. Chauhan, J. Saini, S. Chaudhary, *Nano-Struct. Nano-Objects.*, 2020, **24**, 100585, doi: 10.1016/j.nanoso.2020.100585.
[23] Q. Li, Z. Bai, X. Xi, Z. Guo, C. Liu, X. Liu, X. Zhao, Z. Li, Y. Cheng, Y. Wei, *Spectrochim. Acta Part A.*, 2021, **248**, 119208, doi: 10.1016/j.saa.2020.119208.
[24] G. Jeong, J. M. Lee, J. Lee, J. Praneerad, C. A. Choi, P. Supchocksoonthorn, A. K. Roy, W. Chae, P. Paoprasert, M. K. Yeo, G. Murali, S. Y. Park, D. Lee, I. In, *Appl. Surf. Sci.*, 2021, **542**, 148471, doi: 10.1016/j.apsusc.2020.148471.
[25] R. Atchudan, T. N. J. I. Edison, S. Perumal, N. Muthuchamy, Y. R. Lee, *Fuel*, 2020, **275**, 117821, doi: 10.1016/j.fuel.2020.117821.
[26] K. Zhang, P. Sun, M. C. A. S. Faye, Y. Zhang, *Carbon*, 2018, **130**, 730-740, doi: 10.1016/j.carbon.2018.01.036.
[27] M. Xue, M. Zou, J. Zhao, Z. Zhan, S. Zhao, *J. Mater. Chem. B.*, 2015, **3**, 6783-6789, doi: 10.1039/C5TB01073J.
[28] A. Prasannan, T. Imae, *Ind. Eng. Chem. Res.*, 2013, **52**, 15673–15678, doi: 10.1021/ie402421s.
[29] P. Huang, S. Xu, M. Zhang, W. Zhong, Z. Xiao, Y. Luo, *Phys. Chem. Chem. Phys.*, 2019, **21**, 26133-26145, doi: 10.1039/C9CP04880D.
[30] S. Pandiyan, L. Arumugam, S. P. Srirengan, R. Pitchan, P. Sevugan, K. Kannan, G. Pitchan, T. A. Hegde, V. Gandhirajan, *ACS Omega*, 2020, **5**, 30363–30372, doi: 10.1021/acsomega.0c03290.
[31] A. Pramanik, S. Biswas, P. Kumbhakar, *Spectrochim. Acta Part A*, 2018, **191**, 498-512, doi: 10.1016/j.saa.2017.10.054.
[32] A. Pramanik, S. Biswas, A. K. Kole, C. S. Tiwary, R. N. Krishnaraj, P. Kumbhakar, *RSC Adv.*, 2016, **6**, 99060-99071, doi: 10.1039/C6RA20442B.
[33] S. Khan, A. Gupta, N. C. Verma, C. K. Nandi, *Nano Lett.*, 2015, **15**, 8300–8305, doi: 10.1021/acs.nanolett.5b03915.
[34] V. I. Stsiapura, S. A. Kurhuzenkau, V. A. Kuzmitsky, O. V. Bouganov, S. A. Tikhomirov, *J. Phys. Chem. A*, 2016, **120**, 5481–5496, doi: 10.1021/acs.jpca.6b02577.
[35] M. Zheng, Y. Li, Y. Zhang, Z. Xie, *RSC Adv.*, 2016, **6**, 83501-83504, doi: 10.1039/C6RA16055G.
[36] A. Sciortino, E. Marino, B. Dam, P. Schall, M. Cannas, F. Messina, *J. Phys. Chem. Lett.*, 2016, **7**, 3419–3423, doi: 10.1021/acs.jpclett.6b01590.
[37] P. Kumar, H.B. Bohidar, *J. Lumin.*, 2013, **141**, 155-161, doi: 10.1016/j.jlumin.2013.02.043.
[38] Y. Song, S. Zhu, S. Xiang, X. Zhao, J. Zhang, H. Zhang, Y. Fu, B. Yang, *Nanoscale*, 2014, **6**, 4676-4682, doi: 10.1039/C4NR00029C.
[39] S. K. Cushing, M. Li, F. Huang, N. Wu, *ACS Nano*, 2014, **8**, 1002–1013, doi: 10.1021/nn405843d.
[40] H. A. Nguyen, I. Srivastava, D. Pan, M. Gruebele, *ACS Nano*, 2020, **14**, 6127–6137, doi: 10.1021/acsnano.0c01924.
[41] W. Kong, H. Wu, Z. Ye, R. Li, T. Xu, B. Zhang, *J. Lumin.*, 2014, **148**, 238-242, doi: 10.1016/j.jlumin.2013.12.007.
[42] C. Zheng, X. An, J. Gong, *RSC Adv.*, 2015, **5**, 32319-32322, doi: 10.1039/C5RA01986A.
[43] S. D. Choudhury, J. M. Chethodil, P. M. Gharat, P.K. Praseetha, H. Pal, *J. Phys. Chem. Lett.*, 2017, **8**, 1389–1395, doi: 10.1021/acs.jpclett.7b00153.
[44] X. Jia, J. Li, E. Wang, *Nanoscale*, 2012, **4**, 5572-5575, doi: 10.1039/C2NR31319G.
[45] N. Basu, D. Mandal, *J. Phys. Chem. C*, 2018, **122,** 18732–18741, doi: 10.1021/acs.jpcc.8b04601.
[46] C. J. Reckmeier, Y. Wang, R. Zboril, A. L. Rogach, *J. Phys. Chem. C*, 2016, **120**, 10591–10604, doi: 10.1021/acs.jpcc.5b12294.
[47] E. A. Stepanidenko, I. A. Arefina, P. D. Khavlyuk, A. Dubavik, K. V. Bogdanov, D. P. Bondarenko, S. A. Cherevkov, E. V. Kundelev, A. V. Fedorov, A. V. Baranov, V. G. Maslov, E. V. Ushakova, A. L. Rogach, *Nanoscale*, 2020, **12**, 602-609, doi: 10.1039/C9NR08663C.
[48] K. Sato, R. Sato, Y. Iso, T. Isobe, *Chem. Commun.*, 2020, **56**, 2174-2177, doi: 10.1039/C9CC09333H.
[49] F. Arshad, A. Pal, M. A. Rahman, M. Ali, J. A. Khan, M. P. Sk, *New J. Chem.*, 2018, **42**, 19837-19843, doi: 10.1039/C8NJ03698E.
[50] K. Hola, A. B. Bourlinos, O. Kozak, K. Berka, K. M. Siskova, M. Havrdova, J. Tucek, K. Safarova, M. Otyepka, E. P. Giannelis, R. Zboril, *Carbon*, 2014, **70**, 279-286, doi: 10.1016/j.carbon.2014.01.008.
[51] A. Singh, H. K. Sharma, P. Kaushal, A. Upadhyay, *Afr. J. Food Sci.*, 2014, **5**, 204-215, doi: 10.5897/AJFS2013.1119.

[52] H. Muktha, R. Sharath, N. Kottam, S. P. Smrithi, K. Samrat, P. Ankitha, *BioNanoSci.*, 2020, **10**, 731–744, doi: 10.1007/s12668-020-00741-1.
[53] H. Xue, Y. Chen, X. Liu, Q. Qian, Y. Luo, M. Cui, Y. Chen, DP. Yang, Q. Chen, *Mater. Sci. Eng. C*, 2018, **82**, 197-203, doi: 10.1016/j.msec.2017.08.060.
[54] T. Sarkar, M. Salauddin, R. Chakraborty, *J. Agr. Food Res.*, 2020, **2**, 100081, doi: 10.1016/j.jafr.2020.100081.
[55] P. Mohanty, G. Ayachit, J. N. Mohanty, H. Pandya, A. U. Mankad, J. Das, *Gene Rep.*, 2020, **21**, 100943, doi: 10.1016/j.genrep.2020.100943.
[56] M. Xue, J. Zhao, Z. Zhan, S. Zhao, C. Lan, F. Ye, H. Liang, *Nanoscale*, 2018, **10**, 18124-18130, doi: 10.1039/C8NR05017A.
[57] J. R. Bhamore, S. Jha, T. J. Park, S. K. Kailasa, *J. Photochem. Photobiol. B, Biol.*, 2019, **191**, 150-155, doi: 10.1016/j.jphotobiol.2018.12.023.
[58] M. R. Pacquiao, M. D. G. Luna, N. Thongsai, S. Kladsomboon, P. Paoprasert, *Appl. Surf. Sci.*, 2018, **453**, 192-203. doi: 10.1016/j.apsusc.2018.04.199.
[59] A. Thakur, P. Devi, S. Saini, R. Jain, R. K. Sinha, P. Kumar, *ACS Sustain. Chem. Eng.*, 2019, **7**, 502–512, doi: 10.1021/acssuschemeng.8b04025.
[60] Y. Wang, X. Liu, X. Han, R. Godin, J. Chen, W. Zhou, C. Jiang, J. F. Thompson, K. B. Mustafa, S. A. Shevlin, J. R. Durrant, Z. Guo, J. Tang, *Nat Commun.*, 2020, **11**, 2531, doi: 10.1038/s41467-020-16227-3.
[61] M. Xue, M. Zou, J. Zhao, Z. Zhanab, S. Zhao, *J. Mater. Chem. B*, 2015, **3**, 6783-6789, doi: 10.1039/C5TB01073J.
[62] N. Tokiti, I. Michio, *Bull. Chem. Soc. Jpn.*, 1964, **37**, 1534-1538, doi: 10.1246/bcsj.37.1534.
[63] K. J. Mintz, M. Bartoli, M. Rovere, Y. Zhou, S. D. Hettiarachchi, S. Paudyal, J. Chen, J. B. Domena, P. Y. Liyanage, R. Sampson, D. Khadka, R. R. Pandey, S. Huang, C. C. Chusuei, A. Tagliaferro, R. M. Leblanc, *Carbon*, 2021, **173**, 433-447, doi: 10.1016/j.carbon.2020.11.017.
[64] Y. Liu, N. Xiao, N. Gong, H. Wang, X. Shi, W. Gu, L. Ye, *Carbon*, 2014, **68,** 258-264, doi: 10.1016/j.carbon.2013.10.086.
[65] P. K. Yadav, V. K. Singh, S. Chandra, D. Bano, V. Kumar, M. Talat, S. H. Hasan, *ACS Biomater. Sci. Eng.*, 2019, **5**, 623–632. doi: 10.1021/acsbiomaterials.8b01528.
[66] E. Arkan, A. Barati, M. Rahmanpanah, L. Hosseinzadeh, S. Moradi, M. Hajialyani, *Adv Pharm Bull.*, 2018, **8**, 149-155, doi: 10.15171/apb.2018.018.
[67] W. Meng, X. Bai, B. Wang, Z. Liu, S. Lu, B. Yang, *Energy Environ. Mater.*, 2019, **2**, 172-192, doi: 10.1002/eem2.12038.
[68] T. K. Mondal, S. K. Saha, *ACS Sustainable Chem. Eng.*, 2019, **7**, 19669–19678, doi: 10.1021/acssuschemeng.9b04817.
[69] S. Mei, X. Wei, Z. Hu, C. Wei, D. Su, D. Yang, G. Zhang, W. Zhang, R. Guo, *Opt. Mater.*, 2019, **89**, 224-230, doi: 10.1016/j.optmat.2019.01.021.
[70] A. Mewada, S. Pandey, S. Shinde, N. Mishra, G. Oza, M. Thakur, M. Sharon, M. Sharon, *Mater. Sci. Eng. C*, 2013, **33**, 2914-2917, doi: 10.1016/j.msec.2013.03.018.

Author information

Anjali Vijeata *is currently a Ph.D. Candidate under the supervision of Dr, Savita Chaudhary and Prof. G.R. Chaudhary in the Department of Chemistry Panjab University, Chandigarh, India. She received her master's degree from Kurukshetra University. Her research interests mainly focus on the biomass derived functional nanoparticles and their utilization.*

Ganga Ram Chaudhary *Director SAIF/CIL/UCIM and Senior Professor in Department of Chemistry, Panjab University, Chandigarh. He has made significant contributions in the field of Thermodynamics, Catalysis and Nano chemistry. Prof. Chaudhary is credited with more than 150 publications in international journals of repute with h-index of 24 and is an author of about 10 books/chapters. He has been credited with various precious project including Developed efficient Photo Voltaic (PV) Solar Power Plant and Concentrated Solar Power (CSP) Plants for integrated Electric Vehical charging station and Indo-US Partnership on Green Chemistry/Engineering and Technologies Education. Some of important research work of Prof. Chaudhary include: Synthesis and characterization of metal oxide nanoparticles and its utility for the removal of water contaminants. Recent work belongs to the design of noval metallosurfactants that can be engineered according to the requirement and act as a carrier and template for nanoparticle synthesis. Successful attempt was made to synthesize metallic nanoparticles and used them for the degradation of harmful toxins.*

Ahmad Umar *received his Ph.D. in semiconductor and chemical engineering from Chonbuk National University, South Korea. He worked as a research scientist in Brain Korea 21, Centre for Future Energy Materials and Devices, Chonbuk National University, South*

Korea, in 2007–2008. Afterwards, he joined the Department of Chemistry in Najran University, Najran, Saudi Arabia. He is a distinguished professor of chemistry and served as deputy director of the Promising Centre for Sensors and Electronic Devices (PCSED), Najran University, Najran, Saudi Arabia. Professor Ahmad Umar is specialized in 'semiconductor nanotechnology', which includes growth, properties and their various high technological applications, for instance, gas, chemicals and biosensors, optoelectronic and electronic devices, field effect transistors (FETs), nanostructure-based energy-harvesting devices, such as solar cells, Li-ion batteries, super-capacitors, semiconductor nanomaterial- based environmental remediation, and so on. He is also specialized in the modern analytical and spectroscopic techniques used for the characterizations and applications of semiconductor nanomaterials. He contributed to the world of science by editing world's first handbook series on Metal Oxide Nanostructures and Their Applications (5-volume set, 3500 printed pages, www.aspbs.com/mona) and handbook series on Encyclopedia of Semiconductor Nanotechnology (7-volume set; www.aspbs.com/esn), both published by American Scientific Publishers (www.aspbs.com). He has published more than 600 research papers in reputed journal with h-index of 75 and i10-index of 377 with total citations of 20221 (According to Google scholar).

Savita Chaudhary *received her B.Sc, M.Sc and Ph.D. degrees in Chemistry from the Panjab University in Chandigarh, India. Dr. Chaudhary has published over 115 research articles in peer-reviewed international journals and 8 book chapters. She was awarded the DST-DAAD PPP fellowships in 2008. She is an editorial member of the International Journal of Chemistry and Chemical Engineering (IJCCE) and Advanced Science, Engineering, and Medicine. Dr. Chaudhary is specialized in the synthesis, growth, properties, and applications of engineered nanostructures in the areas of gas, luminescent and biosensors, environmental remediation, catalysis, and photocatalysis. She has made significant contributions in the fields of surfactant chemistry and nanochemistry. Her recent work focuses on the design of different types of nanoparticles possessing higher biocompatibility applicable as carrier for herbicides.*